Available online at www.sciencedirect.com
ScienceDirect
Trans. Nonferrous Met. Soc. China 30(2020) 110−122
Transactions of Nonferrous Metals Society of China
www.tnmsc.cn

Effects of punch velocity on microstructure and tensile properties of thixoforged Mg_2Si_p/AM60B composite

Su-qing ZHANG[1,2], Ti-jun CHEN[1], Ji-xue ZHOU[2]

1. State Key Laboratory of Advanced Processing and Recycling of Nonferrous Metals, Lanzhou University of Technology, Lanzhou 730050, China;
2. Shandong Provincial Key Laboratory of High Strength Lightweight Metallic Materials, Qilu University of Technology (Shandong Academy of Science), Ji'nan 250014, China

Received 18 December 2018; accepted 25 November 2019

Abstract: The effects of punch velocity on the microstructures and tensile properties of Mg_2Si_p/AM60B composite were investigated. In comparison, the tensile properties of the permanent mold casting of this composite were also analyzed. The results indicate that the punch velocity obviously influences the microstructure through changing the secondary solidification behaviors and semisolid deformation mechanisms. The variations of the microstructures and deformation mechanisms are responsible for the changes in tensile properties and fracture modes of the composites. The best comprehensive tensile properties of this composite are obtained under the punch velocity of 60 mm/s. The resulting ultimate tensile strength and elongation of the composite are found to be 198 MPa and 10.2%, respectively. The excellent tensile properties of the thixoforged composite are ascribed to the elimination of porosities and the work hardening.

Key words: thixoforging; semisolid deformation; fracture mechanism; strengthening mechanism

1 Introduction

Magnesium alloys have been receiving more and more attentions in the field of automobile, electronic products, portable tools, sporting goods and aerospace vehicles in recent years, because they possess high specific toughness and strength, good damping capacity and machinability, and so on [1]. However, insufficient strength at high temperatures, low wear and creep resistance of the magnesium alloys limit their extensive applications [2]. Magnesium-based composites combining the properties of magnesium alloys and ceramics, are considered as the most promising way to overcome these shortcomings of magnesium alloys [1,3,4]. The in-situ synthesis technology produces the desired reinforcements via reaction in molten alloy during traditional cast [5], which is a promising solution to those shortcomings of magnesium alloy. In the previous investigation, fine-grain in-situ Mg_2Si_p/AM60B composite has been achieved via traditional casting technique by additions of 0.5 wt.% Sr and 0.2 wt.% SiC_p [6]. The reinforcements of Mg_2Si particles with grain size of 20−40 μm were uniformly distributed in the AM60B alloy matrix. Unfortunately, the existence of porosities deteriorates the mechanical properties of this composite excessively, not meeting the requirements of industry applications. Thus, it is essential to develop an effective approach to take full advantage of this composite.

Foundation item: Project (51804190) supported by the National Natural Science Foundation of China; Project (ZR2017LEM001) supported by Shandong Provincial Natural Science Foundation, China; Project (2017CXGC0404) supported by Shandong Province Key Research and Development Plan, China; Project (2019QN0022) supported by the Youth Science Funds of Shandong Academy of Sciences, China

Corresponding author: Ti-jun CHEN; Tel: +86-931-2976573; Fax: +86-931-2976578; E-mail: chentj@lut.cn

DOI: 10.1016/S1003-6326(19)65184-8

Thixoforming, a relatively new metal forming technology, can enhance the mechanical properties of magnesium or/and aluminum alloys through reducing or eliminating shrinkage porosity and gas pores [7−10]. And this technology has been employed in manufacturing magnesium, aluminum alloys and their composites [11−15]. Consequently, it can be theoretically inferred that the combination of the in-situ synthesis technology with thixoforming technology is a good way to fabricate the Mg_2Si_p/AM60B composites with high performance.

Unfortunately, researches on magnesium-based composites relatively lag behind the magnesium alloys [12,16,17]. Moreover, for researchers, the semi-solid deformation is particularly interesting [18]. The deformation in the mushy zone results in the residual stresses in the resultant products, and affects the quality of it dramatically [19,20].

Therefore, it is very urgent to clarify the effects of the processing parameters on microstructure and mechanical properties of the thixoforged magnesium-based composites. This work presents the progress of an ongoing research work on thixoforged in-situ Mg_2Si_p/AM60B composite. The effects of punch velocity on microstructures and tensile properties are investigated. The informative results are compared with those of the permanent mold casting (PMC) of Mg_2Si_p/AM60B composite.

2 Experimental

The in-situ Mg_2Si_p/AM60B composite for thixoforging was prepared by traditional casting technology using commercial AM60B magnesium alloy, pure Mg and commercial Al−30Si master alloy. Mg−30Sr master alloy was used as a modification for the in-situ formed Mg_2Si particles and Mg−25SiC pressed cakes (mixture powder, the sizes of SiC particles and Mg powders were 7 and 40 μm, respectively) were served as grain refiner for primary α-Mg dendrites. The nominal composition of AM60B matrix was 5.5%−6.5% Al, 0.24%−0.6% Mn, ≤0.22% Zn and ≤0.01% Cu. According to the composition of AM60B−2wt.%Si, AM60B alloy, pure Mg and Al−30Si master alloy were melted in an electric resistance furnace at 790 °C, and then 0.5% Sr (using Mg−30Sr master alloy) was added. The melt was then isothermally held for 20 min and 0.2 wt.% SiC_p (using the Mg−25SiC cakes) was introduced. The detail of the processing about the addition for this cakes was introduced in the previous work [21]. Subsequently, the resulting melt was degassed using 1.5% C_2Cl_6 and held for 10 min, and finally poured into a steel mould with a cavity of *d*50 mm × 500 mm. Thus, the as-cast ingot of in-situ AM60B−10vol.%Mg_2Si_p composite was obtained. It has to mention that, a covering agent of RJ-2 designed for magnesium alloys was used for protecting the melt from oxidation during melting.

The casting ingots were machined into rods with dimensions of *d*42 mm × 30 mm as the starting ingots for thixoforging. The rods were reheated in a resistant furnace under argon gas protection at a semisolid temperature of 600 °C for 60 min. The previous investigations indicated that this reheating parameter was adequate for achieving the Mg_2Si_p/AM60B composite with the highest ultimate tensile strength [17−19]. Then, the semisolid rods were quickly transferred into a die with a cavity of *d*50 mm × 45 mm and thixoforged using a hydraulic pressing machine at the punch pressure of 160 MPa. The die was preheated to 300 °C. The employed punch velocities were set to be 20, 40, 60, 80 and 100 mm/s, respectively. In addition, the graphite powder was used as lubricant during thixoforging. By repeating the above experimental process, some thixoforged products under different punch velocities were obtained.

Tensile testing bars were machined by CNC spark-erosion wire cutting machine from the center region of each thixoforged product parallel to the forging pressure. Their dimensions are shown in Fig. 1. The tensile testing was conducted on a universal material testing machine with a loading velocity of 1 mm/s. The average of five testing values was taken as the tensile properties of a thixoforged composite. The metallographic specimens were also cut from the center region of each product and one cross-section parallel to the forging direction was polished by standard metallographic techniques. Subsequently, they were chemically etched using 4% nitric acid ethanol solution and observed on a scanning electron microscope (SEM) and an optical microscope (OM). The compositions of primary particles in the microstructures were examined by energy dispersive spectroscopy (EDS) equipped in the

SEM. For each sample, 20 zones were measured, and the average value was considered as the composition of the sample. The metallographic specimens were then annealed at 430 °C for 60 min and observed again on the optical microscope to analyze the plastic deformation during thixoforging. Some typical fracture surfaces and side-views were also observed on the SEM and OM, respectively.

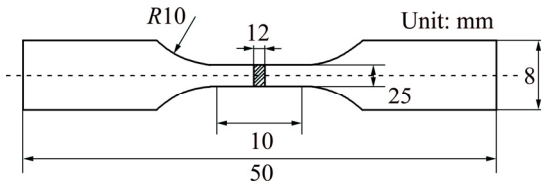

Fig. 1 Schematic of tensile testing specimen

3 Results and discussion

3.1 Semisolid microstructures of composite

For the thixoforging technology, the key procedure is the fabrication of the semisolid ingots [22]. With regard to *d*16 mm composite specimens, the microstructure evolution during partial remelting at 600 °C has been reported in the previous work [23], and the solid fraction change with the temperature has been investigated [24]. Figure 2 presents the microstructures of the composite reheated at 600 °C for 60 min and quickly water-quenched. It can be found that the microstructures in the edge and center regions are all composed of spheroidal primary α-Mg particles, Mg_2Si particles and liquid phase. However, the liquid fraction in the edge region (37 vol.%) is larger than that in the center region (26 vol.%), and the primary α-Mg particles in the edge (~90 μm) are smaller than those in the center (~120 μm). Most of the Mg_2Si particles locate in the intergranular regions, and a few of them present in the liquid pools entrapped within the primary α-Mg particles, as shown in Fig. 2.

The differences in microstructures between the edge and center are common, which could be controlled by adjusting the technological parameters [11−13]. The reasons have been reported in the previous work [23,24]. Although the micro- structures in different regions are not so uniform, the primary α-Mg particles are quite spheroidal and the liquid factions are within the range of 30%−40%. The whole microstructure is appropriate for thixoforging.

3.2 Effects of punch velocity on microstructure and tensile properties of thixoforged composite

3.2.1 Microstructure

Figure 3 shows the microstructures of the composites thixoforged under different punch velocities, which are taken in the center of the specimen. It is indicated that all of the microstructures are composed of the primary α-Mg particles, Mg_2Si particles and secondary solidified structures. The primary α-Mg particles almost connect with each other when the punch velocity is 20 mm/s and the outlines of them are indiscernible (Fig. 3(a)). The secondary solidified structures are only located at some triple points. In addition, a kind of fine grains form in some local regions (marked by A in Fig. 3(a)). The amount of the secondary solidified structures increases as the punch velocity rises, and primary α-Mg particles are gradually separated by further increased secondary solidified structures (Figs. 3(b, c)), but the amount of the fine grains decreases. As the

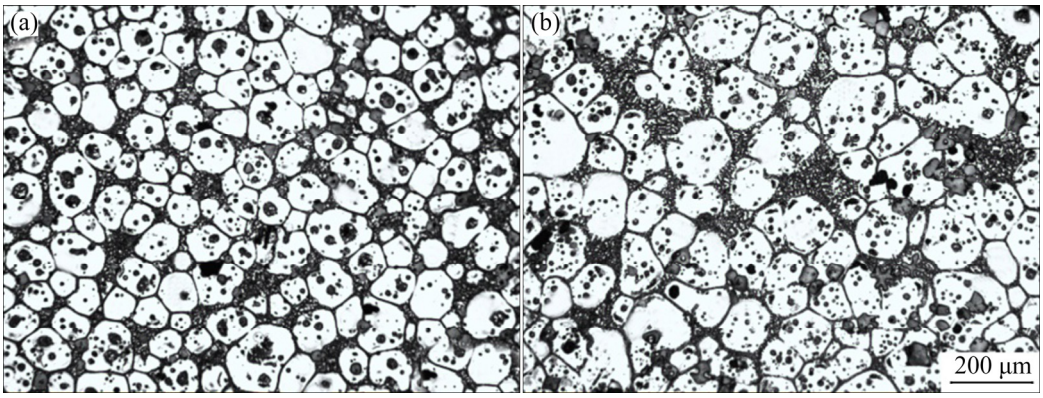

Fig. 2 Semisolid microstructures of composite heated at 600 °C for 60 min in edge (a) and center (b) of ingot

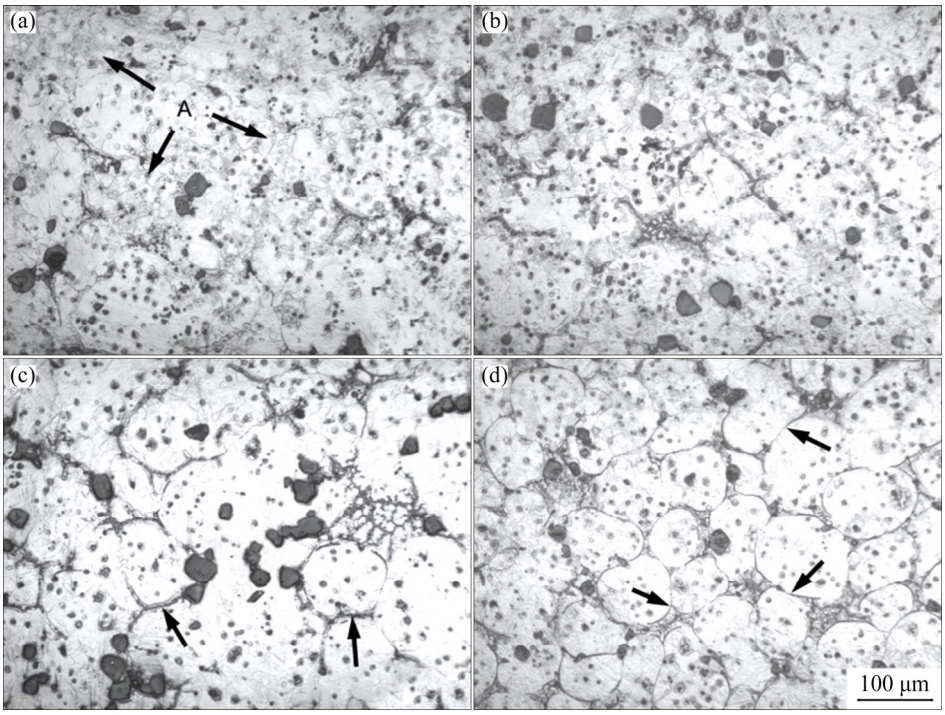

Fig. 3 Microstructures of composites thixoforged under different punch velocities: (a) 20 mm/s; (b) 60 mm/s; (c) 80 mm/s; (d) 100 mm/s

punch velocity reaches 100 mm/s, the microstructure evolves into the individual primary α-Mg particles separated by the secondary solidified structures (Fig. 3(d)).

In order to understand the microstructure under different punch velocities, the solidification process is divided into three stages, as shown in Fig. 4. It should be noted that, the temperature of each stage is estimated, and the time from the punch initiation to touching the ingot is within 5 s.

The first stage begins with the semisolid ingot being taken out of the resistance furnace until the mould cavity is filled up. During this stage, liquid phase solidifies into the secondary primary α-Mg phases (short for SPP in the following) under normal pressure. It is difficult for the SPP to reach the requirement for independent nucleation owing to the relatively high mould temperature of 300 °C. In this case, the SPP preferentially grow up on the surfaces of the primary α-Mg particles, resulting in the original primary α-Mg particles growing up.

The second stage starts with the mould cavity being filled up, and finishes with the punch pressure reaching the setting value (160 MPa). During this stage, the semisolid ingot rapidly reaches the requirement for independent nucleation. Therefore, some of the SPP independently nucleate under

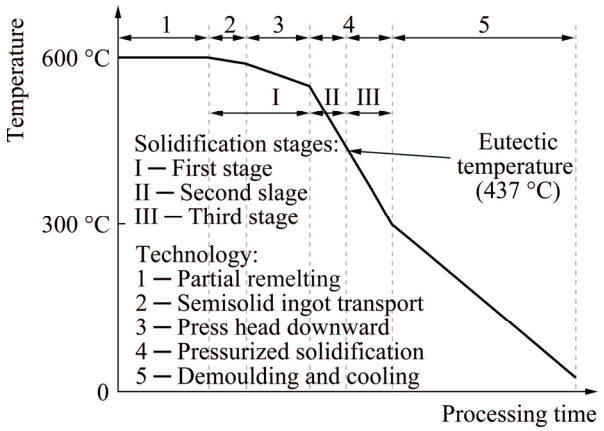

Fig. 4 Schematic of solidification stages during thixoforging

pressure. Of course, part of the SPP precipitating close to the primary α-Mg particles can also directly attach on the surfaces of them. However, owing to the increased solidification rate, the amount of the attached SPP is relatively small.

The third stage is the residual liquid phase solidifying into eutectic structures under the setting pressure. In this stage, the eutectic α-Mg phase preferentially grows up on the surfaces of the surrounding SPP and only eutectic β phase ($Mg_{17}Al_{12}$) is left between the primary α-Mg particles (marked by arrows in Figs. 3(c, d)). That is

to say, the eutectic structures are in a divorced form. Therefore, the SPP can be gradually distinguished from the primary α-Mg particles as the punch velocity increases (comparing Fig. 3(b), (c) and (d) with (a)).

Till now, two theories are tried to explain the effects of pressure on the solidification behavior during thixoforging. The first is the enhanced heat-transfer capability from the pressure. During traditional solidification, the volume of the molten alloy is shrunken. Then, an air gap thereby is formed between the mould and the casting [18], resulting in the decrease in cooling rate. However, the gap can be quickly eliminated under a critical pressure [25−28]. ZHANG et al [25] found that the critical pressure was 80 MPa for the rheo-squeezed AZ91−Ca. ZHANG et al [26] and MASOUMI and HU [27] considered that the mould and the casting completely contacted with each other under the pressure of 90 MPa for squeeze casting AM50. GUO et al [28] reported that the gap was eliminated when the pressure exceeded 70 MPa during rheo-squeezing of A356. In this work, the applied pressure is up to 160 MPa. Therefore, it is reasonable to believe that the gap can be quickly eliminated during the second stage of solidification, resulting in the enhanced heat-transfer, and the cooling rate is thereby increased.

The second is the change of the Mg−Al phase diagram resulting from applied pressure. According to Clausius−Clapeyron equation [29],

$$\frac{\Delta T_{\mathrm{m}}}{\Delta P}=\frac{T_{\mathrm{m}}(V_{\mathrm{l}}-V_{\mathrm{s}})}{\Delta H_{\mathrm{f}}} \tag{1}$$

where T_{m} is the equilibrium solidification temperature, V_{l} is the specific volume of the liquid, V_{s} is the specific volume of the solid, and ΔH_{f} is the latent heat of solidification. By deducing Eq. (1), T_{m} can be expressed as

$$T_{\mathrm{m}}=C\exp(\frac{V_{\mathrm{l}}-V_{\mathrm{s}}}{\Delta H_{\mathrm{f}}}P) \tag{2}$$

where C is a constant.

The effect of pressure P on ΔH_{f} is negligible. Thus, the increase in P results in the increase in T_{m}, and thus induces a larger supercooling compared to traditional casting. Therefore, the nucleation rate is obviously promoted.

Although the contributions of the increased pressure P and cooling rate to the solidification rate have not been calculated, it should also be considered that the synergetic effect from these two factors promotes the solidification rate.

MI et al [30] plotted the Mg−Al binary phase diagram under different pressures (Fig. 5). As shown in Fig. 5, the eutectic point in the Mg−Al equilibrium binary phase diagram moves towards the magnesium-rich side as the pressure increases. That is to say, the solubility of Al in Mg decreases as the pressure increases. Table 1 indicates that the Al content in the center of the α-Mg particles is almost invariant. However, the Al content in the edge of primary α-Mg phase significantly decreases as the punch velocity increases (Table 1). Namely, the Al content in the residual liquid increases with the punch velocity, resulting in the increased amount of the formed eutectic β phase.

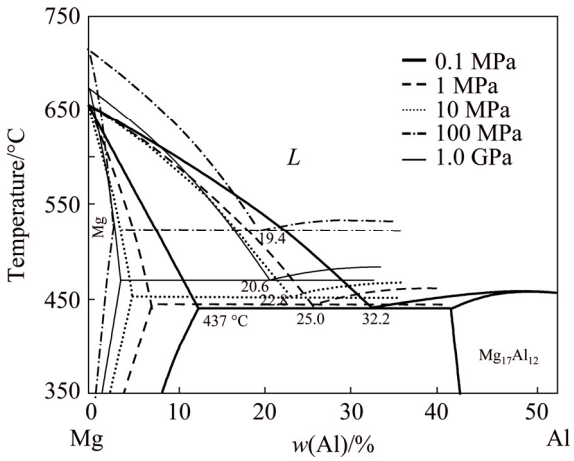

Fig. 5 Mg−Al equilibrium phase diagram under different solidifying pressures [30]

Table 1 Compositions of α-Mg phases under different punch velocities

Punch velocity/(mm·s^{-1})	Location	Composition/wt.%			
		Al	Mg	Si	Sr
20	Center of primary α-Mg	5.5	94.5	0	0
	Edge of primary α-Mg	7.2	92.8	0	0
40	Center of primary α-Mg	5.3	94.3	0.2	0.2
	Edge of primary α-Mg	7.0	92.5	0.2	0.3
60	Center of primary α-Mg	5.4	94.6	0	0
	Edge of primary α-Mg	7.0	92.7	0.1	0.2
80	Center of primary α-Mg	5.5	94.5	0	0
	Secondary α-Mg	6.3	93.7	0	0
100	Center of primary α-Mg	5.3	94.5	0.2	0
	Secondary α-Mg	6.0	93.5	0.3	0.2

Figure 6 indicates that a large number of the eutectic β phases (in white contrast, marked by arrows) are uniformly distributed in the form of small spots when the composites are thixoforged under the punch velocity of 20 mm/s (Fig. 6(a)). As the punch velocity is up to 100 mm/s, most of the β phases distribute in bone shape shape and a halos-like surrounding α-Mg particles. The amount of β phase is significantly increased (by comparing Fig. 6(c) with (a)).

Additionally, the morphology of the SPP also varies as the punch velocity changes (by comparing Fig. 6(b) with (d)). At low punch velocity, the SPP uniformly attach on the surface of primary α-Mg particles (Fig. 6(b)). However, at high punch velocity, irregular SPP attach on the primary α-Mg particles (Fig. 6(d)). The morphological variation is attributed to the change of solidification rate [31]. The increase in the punch velocity results in the increase in solidification rate. Therefore, the solidifying interface is unstable [32−34]. When the SPP grow up on the surface of the primary α-Mg particles, some bulges then form and grow towards the liquid phase to form the irregular secondarily solidified structures. Therefore, the irregular structures are then formed, which results in the poor filling ability. Therefore, the porosities are easily generated in this region (Fig. 7). It can be inferred that these porosities greatly impair the mechanical properties of the composite.

3.2.2 Plastic deformation during thixoforging

As shown in Fig. 3, a kind of small-size grain forms in some local regions (Fig. 3(a)), and gradually disappears as the punch velocity increases (Figs. 3(b, c)). Therefore, it can be suggested that the plastic deformation and recrystallization have occurred during thixoforging and subsequent cooling, which play an important role in the final mechanical properties. In order to analyze the effects of punch velocity on the plastic deformation, the specimens are subjected to annealing treatment at 430 °C for 60 min. If the α-Mg particles are plastically deformed during thixoforging, small grains can be formed through recrystallization during annealing treatment. The larger the deformation degree and the area, the smaller and the more the grains are formed. Figure 8 gives the experimental results. As shown in Fig. 8(a), the α-Mg particles in the thixoforged microstructure evolve into quite uniform fine grains after being annealed. This implies that most of the α-Mg particles are severely deformed during thixoforging

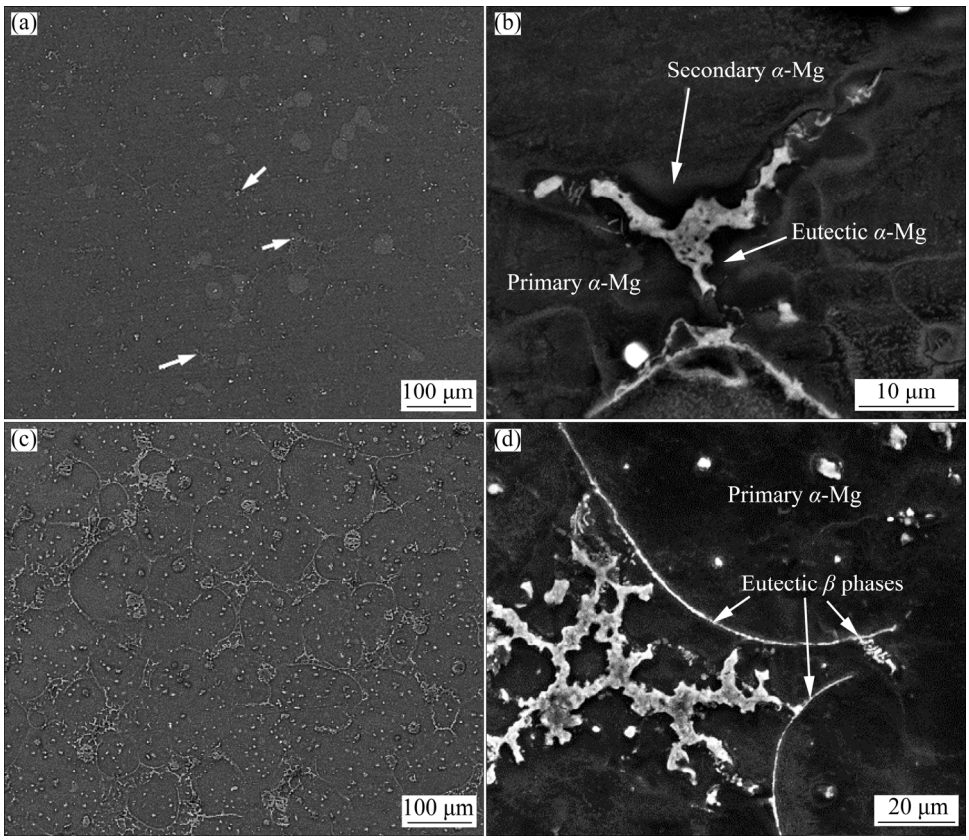

Fig. 6 SEM images of composites thixoforged under different punch velocities: (a, b) 20 mm/s; (c, d) 100 mm/s

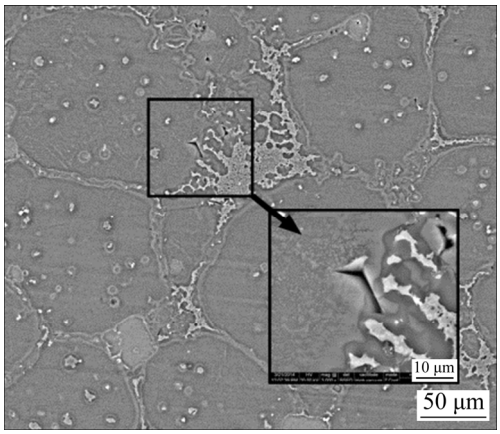

Fig. 7 SEM image showing porosity in secondarily solidified structures thixoforged under 100 mm/s

under the punch velocity of 20 mm/s. As the punch velocity increases, the number of fine grains gradually decreases (by comparing Figs. 8(b) and (c) with (a)). Moreover, the distribution of the fine grains is not uniform. This means that the plastic deformation only occurs at some local regions. When the punch velocity is up to 100 mm/s, the distribution of the small grains is disordered (Fig. 8(d)). It can be suggested that only a few of α-Mg particles are severely deformed.

There are four mechanisms for the semisolid ingot deformation: liquid flow (LF), flow of liquid incorporating solid particles (FLS), sliding between solid particles (SS) and plastic deformation of solid particles (PDS) [35,36]. These mechanisms are usually conducted in the sequence of LF, FLS, SS and PDS. The former two operate when the solid particles are surrounded by the liquid phase and the latter two occur when the solid particles contact with each other [36].

As mentioned above, when the punch velocity is 20 mm/s, the amount of the attached SPP is the largest, and the residual liquid is the least. In this case, the deformation of the semisolid ingot is easily through SS and PDS mechanisms. Therefore, the plastic deformation is operated. As a result, many small grains are generated after the composite is annealed (Fig. 8(a)).

With the increase in punch velocity, the growth rate of grains decreases and the fraction of residual liquid phase increases, which results in the decreased contacting among the primary particles. The proportion of the deformation operated through LF and FLS is increased. So, both of the range and degree of plastic deformation are decreased. As a result, the grain size in the annealed composite is

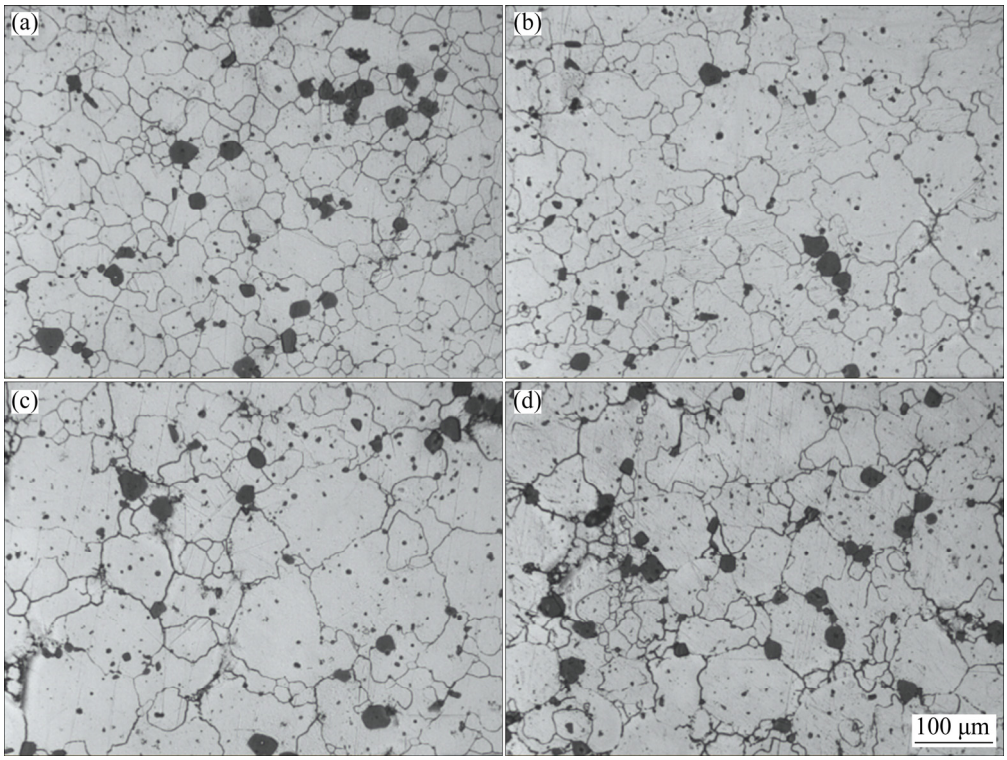

Fig. 8 Annealed microstructures of composites thixoforged under different punch velocities: (a) 20 mm/s; (b) 60 mm/s; (c) 80 mm/s; (d) 100 mm/s

then increased (Figs. 8(b,c)). However, when the punch velocity exceeds a certain value, the situation is reversed. The response time of the deformation mechanism decreases in the sequence of LF, FLS, SS and PDS [35,36]. When the punch velocity reaches 100 mm/s, there may be no enough time to realize the deformation through the LF, FLS and SS modes. This means that the deformation has to operate in the PDS mechanism. Thus, the plastic deformation degree increases. However, the plastic deformation is not so uniform because the deformation rate in the semisolid ingot is not so uniform. Thus, the distribution of these small grains is also disordered and unsystematic (Fig. 8(d)).

3.2.3 Tensile properties

Figure 9 presents the variations of tensile properties of thixoforged composites with punch velocity. It is shown that the ultimate tensile strength (UTS) slightly decreases as the punch velocity increases from 20 to 60 mm/s and then sharply decreases with the punch velocity further increasing. The elongation first increases to a peak value at the punch velocity of 60 mm/s and then also decreases. Although the composite thixoforged under 20 mm/s has the highest UTS, in view of the elongation, the punch velocity of 60 mm/s is the optimal parameter for this composite. The UTS of 198 MPa and elongation of 10.2% can be obtained at this punch velocity.

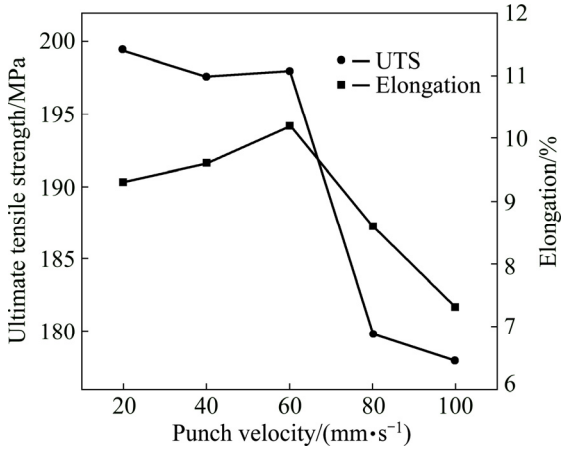

Fig. 9 Variations of tensile properties with punch velocity

Figure 10 shows the fractographs of the composites thixoforged under different punch velocities. The fracture surface of the composite thixoforged under 20 mm/s is characterized by the irregular particles and pits. The side view of the fracture surface, shown in Fig. 11(a), indicates that the cracks either propagate among the α-Mg particles (marked by A) or occasionally traverse them, passing across the black structures within the α-Mg particles (marked by B). This implies that the fracture of this composite belongs to a mixture of transgranular and intergranular modes. Both the irregular particles and pits on the fracture surface are originated from the crack propagation among the α-Mg particles. When the punch velocity is 20 mm/s, the feeding ability is the worst. Therefore, the porosities are easily formed in the last solidified structures, i.e., among the α-Mg particles or/and between the α-Mg particles and Mg_2Si particles. So, the cracks are easy to initiate and propagate in these regions, resulting in the irregular particles and pits on the fracture surface. The black structures within the α-Mg particles originate from the solidifying of the liquid pools entrapped within the primary α-Mg particles. There is no extra liquid to feed the solidification shrinkage. So, these black structures are also the weak sites of the composite. In addition, the semisolid deformation of this composite is in PDS mechanism. The plastic deformation of the α-Mg particles effectively strengthens the matrix through work hardening mechanism [37]. Owing to the feature of work hardening, the relatively high UTS is obtained at the cost of the decrease in elongation (Fig. 9).

Figure 10(b) shows that the irregular particles and pits on the fracture surface are displaced by the dimples. The cracks propagate completely through the α-Mg particles and frequently pass the black structures (mark by arrows in Fig. 11(b)). That is to say, the fracture transforms into the intergranular mode. The increase in the punch velocity results in the more liquid phases solidifying at high pressure. Therefore, the feeding ability is promoted and the liquid phases are squeezed to the last solidified regions under the high pressure. The porosities are thereby reduced. As a result, the cracks propagate through the α-Mg particles. The irregular particles and pits on the fracture surface disappear (Fig. 10(b)). In addition, the FLS mechanism becomes more dominated as the punch velocity increases. The plastic deformation of the α-Mg particles is reduced. The decrease in work hardening is responsible for the decrease in UTS and increase in elongation (Fig. 9) when the punch velocity increases from 20 to 60 mm/s.

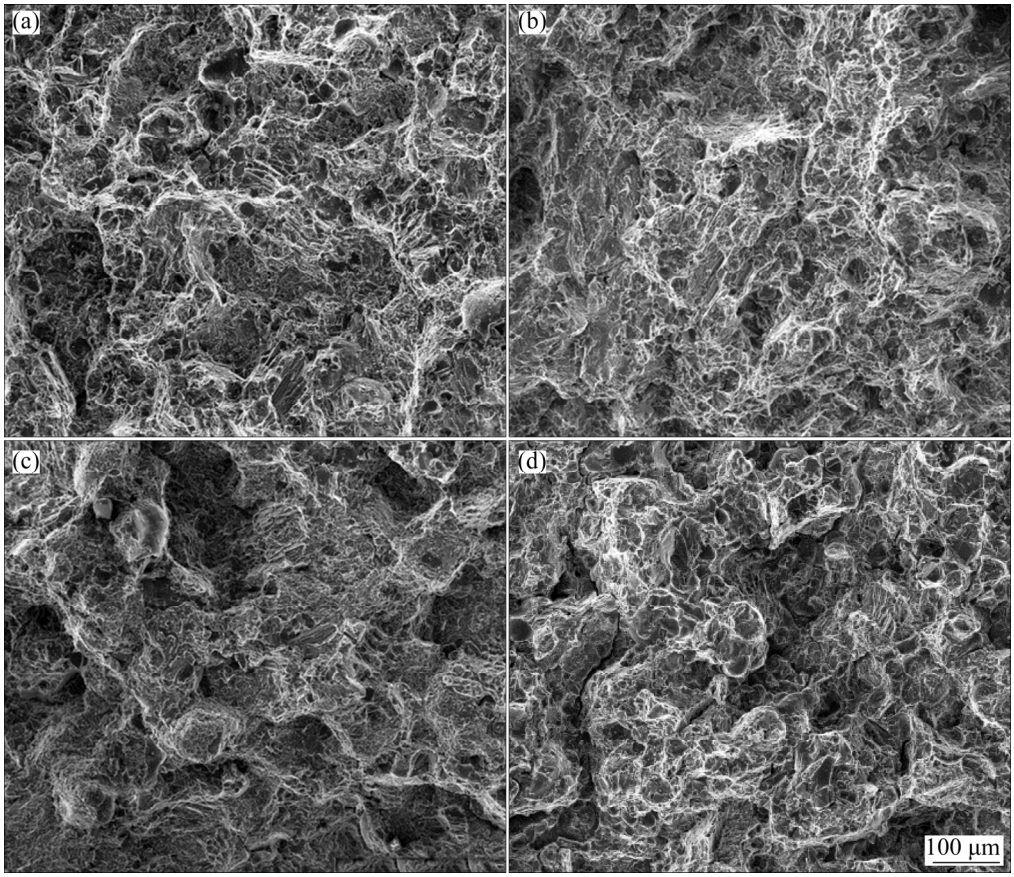

Fig. 10 Fractographs of composites thixoforged under different punch velocities: (a) 20 mm/s; (b) 60 mm/s; (c) 80 mm/s; (d) 100 mm/s

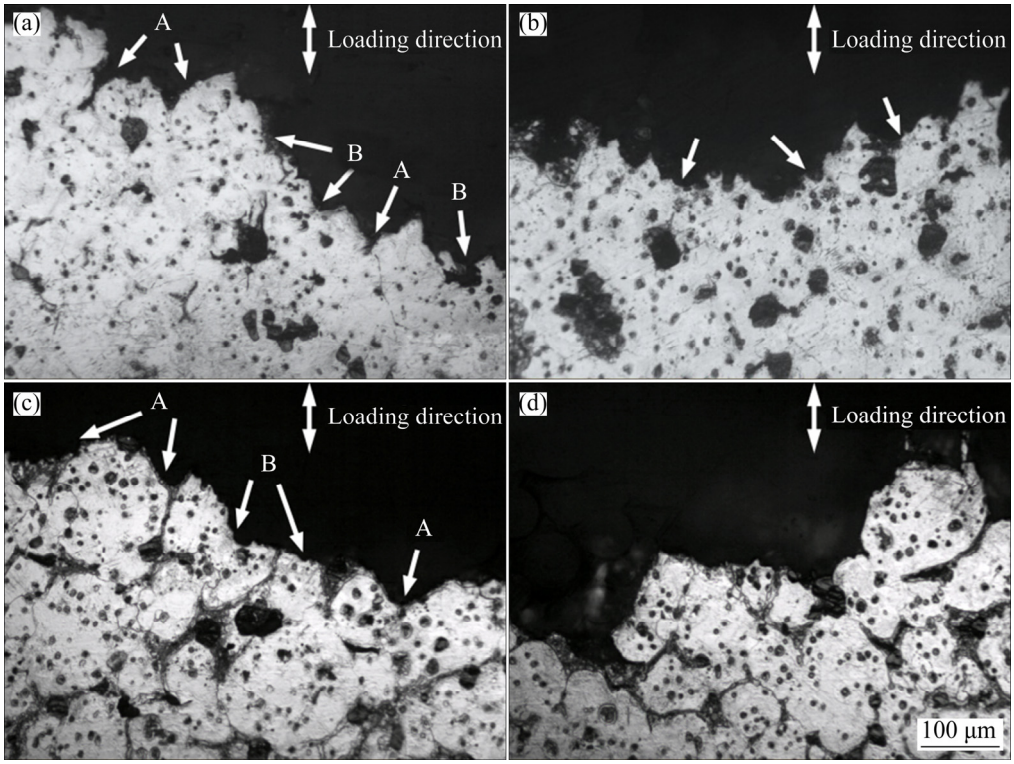

Fig. 11 Side-views of fracture surfaces of composites thixoforged under different punch velocities: (a) 20 mm/s; (b) 60 mm/s; (c) 80 mm/s; (d) 100 mm/s

However, as the punch velocity further increases, the irregular particles and pits on the fracture surface appear again (Fig. 10(c)). The side view of the fracture surface indicates that the fracture of the composite turns into a mixture of transgranular and intergranular modes again (Fig. 11(c)). As mentioned in Section 3.2.2, the increase in punch velocity results in the increase in the amount of eutectic β phases, which separate the α-Mg particles from each other. Since the eutectic β phase belongs to a hard and fragile phase, such distribution of β phases results in the weak bonding strength among the α-Mg particles. Thus, the α-Mg particles are easily debonded during tensile testing. Therefore, the decrease in tensile properties (Fig. 9) and the feature of fracture surface are attributed to the increase in the amount and size of eutectic β phase.

The fracture surface of the composite thixoforged under 100 mm/s is characterized by porosity feature (Fig. 10(d)), and the side view of the fracture surface indicates that the fracture transforms into completely intergranular mode (Fig. 11(d)). As the punch velocity increases, the liquid phases tend to form the irregular structures (Fig. 5(d)), and the porosities are easily generated in the secondarily solidified structures (Fig. 7). Thus, the cracks thereby initiate from these porosities and develop along the secondarily solidified structures. So, the incompact secondarily solidified microstructures result in the inferior tensile properties and the morphological feature on fracture surface of this composite (Fig. 9).

3.2.4 Comparison with PMC composite and strengthening role of Mg_2Si particles

The tensile properties of the permanent mold casting (PMC) composite are investigated. The results exhibit relatively inferior properties, UTS of 108 MPa and elongation of 5%, respectively. In comparison, the tensile properties of the thixoforged composite under punch velocity of 60 mm/s are increased by 83% in UTS and by 110% in elongation, respectively. Figure 12 reveals the fracture surface and its side view of the PMC composite. As shown in Fig. 12(a), the fracture surface of the PMC composite is characterized by obvious porosity feature. The previous work [38] indicated that porosity percentage was reduced from 4% in the PMC composite to 0.15% in the thixoforged composite. These porosities always exist in the last solidified regions, i.e., the eutectic structures among the primary α-Mg dendrites. During tensile testing, the cracks initiate from these porosities and propagate along the eutectic structures. As displayed in Fig. 12(b), the fracture of the PMC composite belongs to typical intergranular mode. Therefore, the super properties of the thixoforged composite are primarily due to the decrease of porosities. In addition, the thixoforged composites are subjected to a certain degree of plastic deformation. Thus, the work hardening also contributes to the improvement of the tensile properties of the thixoforged composite as discussed above.

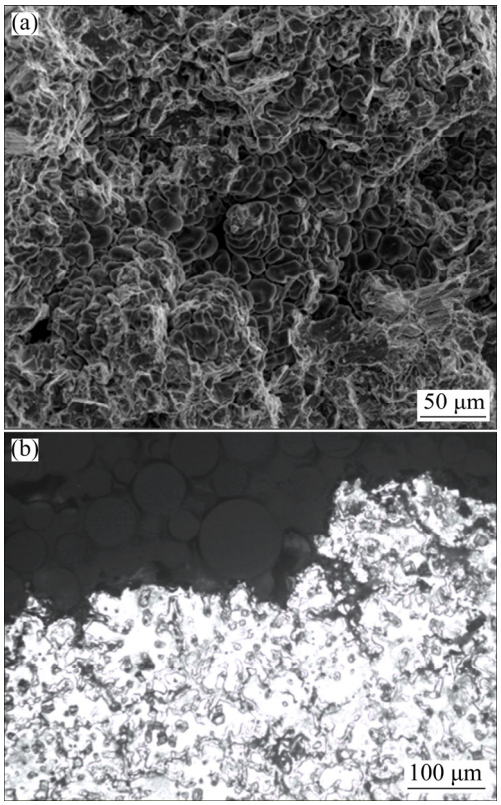

Fig. 12 SEM images of PMC composite: (a) Fracture surface; (b) Side view

The strengthening mechanisms of the Mg_2Si particles have been stated in the previous works [31,38,39]. It is indicated that the reinforcement effect of the Mg_2Si particles changes with the variations of process parameters. Therefore, the effects of punch velocity should also be investigated. Some typical fracture surfaces are shown in Fig. 13. As shown in Fig. 13(a), the interfacial Mg_2Si/matrix debonding is the main damage pattern of the Mg_2Si particles in the

composite thixoforged under 20 mm/s. As the punch velocity increases to 60 mm/s, the Mg_2Si particles break up into pieces (Fig. 13(b)). However, as the punch velocity is up to 100 mm/s, the Mg_2Si particles are seldom found on the fracture surface (Fig. 10(d)).

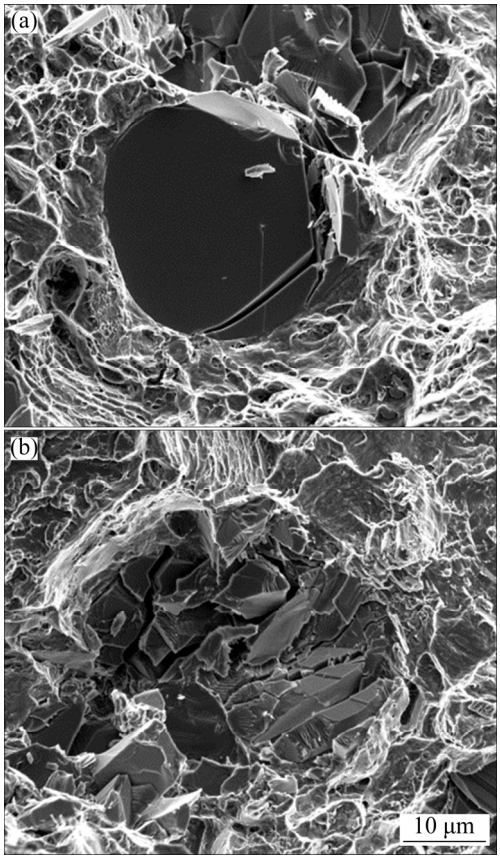

Fig. 13 SEM images showing Mg_2Si particles on fracture surface of composite thixoforged under different punch velocities: (a) 20 mm/s; (b) 60 mm/s

As shown in Fig. 3 and Fig. 8, Mg_2Si particles do not fracture during thixoforging. As mentioned above, the relatively severe plastic deformation occurs when the composite is thixoforged under the punch velocity of 20 mm/s. In this case, the residual stress preferentially concentrates near the interface of Mg_2Si/matrix. During tensile testing, the interfacial debonding is easily operated. When the punch velocity increases to 60 mm/s, the plastic deformation and residual stress during thixoforging decrease. However, during tensile testing, a large concentration of stress is also generated near the interface, due to the difference in mechanical behavior between Mg_2Si particles and the α-Mg matrix. As the strain increases, this stress concentration can increase up to 2−4 times higher than that of the surrounding matrix [40], and finally results in the fragmentation of Mg_2Si particle. When the punch velocity increases to 100 mm/s, the cracks initiate from the porosities in the secondarily solidified structures during tensile testing of the resulting composite and propagate to the secondarily solidified structure. In this case, the Mg_2Si particle has almost no strengthening role in the matrix, and they are seldom found on the fracture surface (Fig. 10(d)).

In summary, the punch velocity obviously influences the strengthening role of the Mg_2Si particles. The high residual stress concentration near the interface of Mg_2Si/matrix and the porosities in the matrix bring a negative influence on the strengthening mechanism of Mg_2Si particle. These should be avoided through adjusting the process parameters.

4 Conclusions

(1) The solidification of Mg_2Si_p/AM60B composite can be divided into three stages. The variation of punch velocity results in the change of the proportion of the microstructures formed under different stage. Increase in punch velocity results in the more liquids solidifying under pressure. Thus, the fractions of the secondarily solidified structures formed under normal or high pressure are changed. The solidification behaviors, composition and morphology of the resulting phases are thereby changed.

(2) When the punch velocity increases from 20 to 100 mm/s, the dominating semisolid deformation mechanisms transform from PDS mode into FLS, and finally into PDS again. The plastic deformation of the semisolid ingot during thixoforging and incomplete recrystallization are responsible for the formation of fine grains and twin planes.

(3) The appropriate punch velocity is 60 mm/s. The corresponding UTS and elongation are 198 MPa and 10.2%, respectively. As the punch velocity increases from 20 to 60 mm/s, the decrease in UTS and the increase in elongation are attributed to the reduced work hardening. The inferior tensile properties are resulted from the eutectic β phases and the formation of porosities in secondarily solidified structures.

(4) The fracture mode of the composites transfers in sequence from a mixture of

intergranular and transgranular modes to a transgranular mode and finally an intergranular mode as the punch velocity increases from 20 to 100 mm/s.

(5) Compared with the PMC composite, UTS and the elongation of the thixoforged composite increase by 83% and 110%, respectively. The excellent tensile properties of the thixoforged composite are ascribed to the elimination of porosities and the work hardening.

References

[1] CHEN L, YAO Y. Processing, microstructures, and mechanical properties of magnesium matrix composites: A review [J]. Acta Metallurgica Sinica (English Letters), 2014, 27(5): 762−774.

[2] HAO Y A, CHEN T J, MA Y, LI Y D, YAN F Y, HUANG X F. Some key issues and accesses to the application of magnesium alloys [J]. International Journal of Modern Physics B, 2010, 24(15−16): 2237−2242.

[3] SHEN M J, WANG X J, YING T, WU K, SONG W J. Characteristics and mechanical properties of magnesium matrix composites reinforced with micron/submicron/nano SiC particles [J]. Journal of Alloys and Compounds, 2016, 686: 831−840.

[4] YE H, LIU X. Review of recent studies in magnesium matrix composites [J]. Journal of Materials Science, 2004, 39(20): 6153−6171.

[5] SAHOO B N, PANIGRAHI S K. Synthesis, characterization and mechanical properties of in-situ (TiC-TiB_2) reinforced magnesium matrix composite [J]. Materials and Design, 2016, 109(5): 300−313.

[6] SHEN Le, CHEN Te-jun, MA Ying, LIU Ming-wei, HAO Yuan. Modification of in-situ Mg_2Si/AM60B magnesium matrix composites with $MgCO_3$ and Sr [J]. Special Casting and Nonferrous Alloys, 2011, 31(7): 653−655. (in Chinese)

[7] TZIMAS E, ZAVALIANGOS A. Materials selection for semisolid processing [J]. Materials and Manufacturing Processes, 1999, 14(2): 217−230.

[8] KIRKWOOD D H. Semisolid metal processing [J]. International Materials Reviews, 1994, 39(5): 173−189.

[9] ATKINSON H V. Semisolid processing of metallic materials [J]. Materials Science and Technology, 2010, 26(12): 1401−1413.

[10] FLEMINGS M C. Behavior of metal alloys in the semisolid state [J]. Metallurgical and Materials Transactions A, 1991, 22(5): 957−981.

[11] CHEN Q, CHEN G, JI X, HAN F, ZHAO Z, WAN J, XIAO X. Compound forming of 7075 aluminum alloy based on functional integration of plastic deformation and thixoformation [J]. Journal of Materials Processing Technology, 2017, 246: 167−175.

[12] CHEN G, ZHANG S, ZHANG H, HAN F, WANG G, CHEN Q, ZHAO Z. Controlling liquid segregation of semi-solid AZ80 magnesium alloy by back pressure thixoextruding [J]. Journal of Materials Processing Technology, 2018, 259: 88−95.

[13] CHEN G, CHEN Q, QIN J, DU Z. Effect of compound loading on microstructures and mechanical properties of 7075 aluminum alloy after severe thixoformation [J]. Journal of Materials Processing Technology, 2016, 229: 467−474.

[14] DEEPAK KUMAR S, MANDAL A, CHAKRABORTY M. Effect of thixoforming on the microstructure and tensile properties of A356 alloy and A356-5TiB_2 in-situ composite [J]. Transactions of the Indian Institute of Metals, 2015, 68(S2): 123−130.

[15] DEEPAK KUMAR S, MANDAL A, CHAKRABORTY M. On the age hardening behavior of thixoformed A356–5TiB_2 in-situ composite [J]. Materials Science and Engineering A, 2015, 636: 254−262.

[16] GADOW R. Lightweight engineering with advanced composite materials−Ceramic and metal matrix composites [J]. Advances in Science and Technology, 2006, 50: 163−173.

[17] LLOYD D J. Particle reinforced aluminium and magnesium matrix composites [J]. International Materials Reviews, 1994, 39(1): 1−23.

[18] PHILLION A B. Recent experimental and numerical developments in semisolid deformation [J]. JOM, 2014, 66(8): 1406−1407.

[19] SMITH L F, KRAWITZ A D, CLARKE P, SAIMOTO S, SHI N, ARSENAULT R J. Residual stresses in discontinuous metal matrix composites [J]. Materials Science and Engineering A, 1992, 159: 13.

[20] MORALES A G, LOPEZ U F. Residual stresses in injection molded products [J]. Journal of Materials Science, 2014, 49(13): 4399−4415.

[21] ZHANG S, CHEN T, LI P. Microstructure and tensile properties of in situ Mg_2Si_p/AM60B composite prepared by thixoforging technology [J]. Journal of Materials Research, 2016, 31(6): 783−796.

[22] FAN Z. Semi-solid metal processing [J]. International Materials Reviews, 2002, 47(2): 47−85.

[23] ZHANG S, CHEN T, CHENG F, LI L. Microstructural evolution and phase transformation during partial remelting of in-situ Mg_2Si_p/ AM60B composite [J]. Transactions of Nonferrous Metals Society of China, 2016, 26(6): 1564−1573.

[24] ZHANG S, CHEN T, LI P, LI L. Semisolid microstructural evolution of fine grain in situ Mg_2Si_p/AM60B composite in mushy zone [J]. Materials Research Innovations, 2015, 19(S10): 44−48.

[25] ZHANG Y, WU G, LIU W, ZHANG L, PANG S, DING W. Microstructure and mechanical properties of rheo-squeeze casting AZ91−Ca magnesium alloy prepared by gas bubbling process [J]. Materials and Design, 2015, 67: 1−8.

[26] ZHANG Q, MASOUMI M, HU H. Influence of applied pressure on tensile behaviour and microstructure of squeeze cast Mg alloy AM50 with Ca addition [J]. Journal of Materials Engineering and Performance, 2012, 21(1): 38−46.

[27] MASOUMI M, HU H. Influence of applied pressure on microstructure and tensile properties of squeeze cast magnesium Mg−Al−Ca alloy [J]. Materials Science and Engineering A, 2011, 528: 3589−3593.

[28] GUO H, YANG X, WANG J. Pressurized solidification of semi-solid aluminum die casting alloy A356 [J]. Journal of Alloys and Compounds, 2009, 485: 812−816.
[29] YUE T M, CHADWICK G A. Squeeze casting of light alloys and their composites [J]. Journal of Materials Processing Technology, 1996, 58(2): 302−307.
[30] MI Guang-bao, LI Pei-jie, HE Liang-ju. Residual bond structure analysis of equilibrium phase diagram of Al−Si and Mg−Al alloys under pressure condition [J]. The Chinese Journal of Nonferrous Metals, 2009, 19(12): 2074−2082. (in Chinese)
[31] ZHANG S, CHEN T, CHENG F, LI L. Effects of mould temperature on microstructure and tensile properties of thixoforged Mg_2Si_p/ AM60B in-situ composites [J]. Journal of Alloys and Compounds, 2015, 657: 582−592.
[32] TRIVEDI R. Morphological stability of a solid particle growing from a binary alloy melt [J]. Journal of Crystal Growth, 1980, 48(1): 93−99.
[33] MARTINEZ R A, KARMA A, FLEMINGS M C. Spheroidal particle stability in semisolid processing [J]. Metallurgical and Materials Transactions A, 2006, 37(9): 2807−2815.
[34] TRIVEDI R. Theory of dendritic growth during the directional solidification of binary alloys [J]. Journal of Crystal Growth, 1980, 49(2): 219−232.
[35] CHEN C P, TSAO C Y A. Response of aluminium/graphite composite to deformation in the semi-solid state [J]. Journal of Materials Science, 1996, 31(19): 5027−5031.
[36] CHEN C P, TSAO C Y A. Semi-solid deformation of non-dendritic strictures−I. Phenomenological behavior [J]. Acta Materialia, 1997, 45(5): 1955−1968.
[37] YADAV S, CHICHILI D R, RAMESH K T. The mechanical response of a 6061-T6 Al/Al_2O_3 metal matrix composite at high rates of deformation [J]. Acta Metallurgica et Materialia, 1995, 43(12): 4453−4464.
[38] ZHANG S, CHEN T, CHENG F, LI P. A comparative characterization of the microstructures and tensile properties of as-cast and thixoforged in situ AM60B-10 vol% Mg_2Si_p composite and thixoforged AM60B [J]. Metals, 2015, 5(1): 457−470.
[39] CHEN T, ZHANG S, CHEN Y, LI Y, MA Y, HAO H. Effects of reheating duration on the microstructures and tensile properties of thixoforged in situ Mg_2Si_p/AM60B composites [J]. Acta Metallurgica Sinica, 2014, 27(5): 957−967.
[40] ARSENAULT R J. Strengthening mechanisms in particulate MMC [J]. Scripta Metallurgica, 1991, 25(11): 2617−2621.

压头速度对触变模锻原位 Mg_2Si_p/AM60B 复合材料显微组织与拉伸性能的影响

张素卿[1,2]，陈体军[1]，周吉学[2]

1. 兰州理工大学 省部共建有色金属先进加工与再利用国家重点实验室，兰州 730050；
2. 齐鲁工业大学(山东省科学院) 山东省轻质高强金属材料重点实验室，济南 250014

摘 要：研究压头速度对 Mg_2Si_p/AM60B 复合材料显微组织和拉伸性能的影响，并与金属型铸造复合材料进行对比。结果表明，压头速度通过改变二次凝固行为和半固态变形机制对复合材料的显微组织产生明显影响，显微组织和变形机制的改变使复合材料的拉伸性能和断裂机制发生变化。当压头速度为 60 mm/s 时，复合材料获得最优的综合拉伸性能，抗拉强度和伸长率分别为 198 MPa 和 10.2%。触变成形复合材料的优异性能归因于缺陷的消除和加工硬化。

关键词：触变锻造；半固态变形；断裂机制；强化机制

(Edited by Bing YANG)